ACS OMEGA

Open Access

http://pubs.acs.org/journal/acsodf

Article

Synthesis and Reactivity of an Olefin Metathesis-Catalyzing Ruthenium Complex with a Selenoether Moiety in the Benzylidene Ligand

Tsubasa Kinugawa, Seishu Mitsusada, Naoki Orito, and Takashi Matsuo*

Cite This: *ACS Omega* 2024, 9, 51604−51610

Read Online

ACCESS | Metrics & More | Article Recommendations | Supporting Information

ABSTRACT: A Hoveyda−Grubbs (HG)-type olefin metathesis complex with a selenoether moiety at the terminus of phenoxy moiety was synthesized. The complex showed direct selenium-atom coordination to the ruthenium center, resulting in higher thermodynamic stability compared with the parent HG catalyst. The selenium atom binding enhanced the tolerance to protic solvent molecules in ring-closing metathesis of *N*-tosyldiallylamide and diethyl diallylmalonate, and also in the cross metathesis between 3-butenylbenzoate and methyl acrylate. The large activation enthalpy observed in the reaction with *n*-butyl vinyl ether indicated an increased contribution of the "dissociative mechanism" during the initiation of the catalytic cycle. Introducing coordinative atoms or functional groups at the terminal of the phenoxy moiety is a useful strategy to regulate the thermostability of HG-type olefin metathesis catalysts.

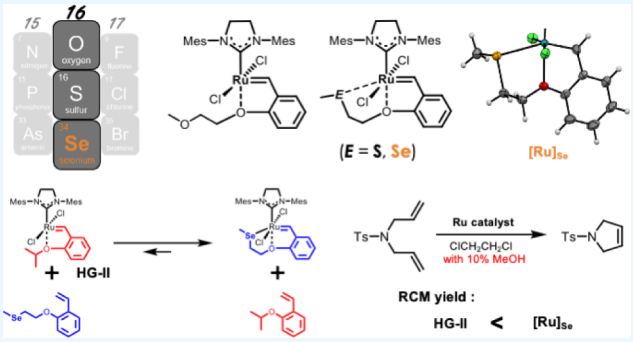

INTRODUCTION

Olefin metathesis (OM) catalyzed by transition metal complexes is a useful method for constructing new olefin moieties through the rearrangement of carbon−carbon double bonds in both laboratory and industrial scale syntheses because OM reactions are highly selective in olefins among various functional groups.[1−4] Hoveyda−Grubbs second generation complex (HG-II (**1**);[5] Chart 1) is the most widely used OM catalyst due to its higher thermostability than other OM transition metal catalysts and ease of functionalization through structural modifications of the *N*-heterocyclic carbenoid (NHC) and benzylidene ligand moieties. These characteristics have led researchers to investigate the applicability of HG-II (**1**) and its derivatives to reactions involving biomolecules in aqueous media.,[2,6,7] Furthermore, several studies have shown that the reactivity of HG-II (**1**) can be modulated by introducing functional groups at the terminal of phenoxy moiety in the complex.[8−11] Coordinative functional groups, such as imide,[12,13] carbonyl,[14,15] and sulfonamide[16] can directly influence the reactivity of the metal center. Additionally, complex **2** regulates the reactivities of the metal center through second coordination sphere effect (i.e., amide-NH ●●● Cl interaction).[17] Replacing the amide group with an ether moiety (complex **3**) led to higher initial velocities in OM reactions compared to those in HG-II (**1**). This is due to electrostatic repulsion between the oxygen and chlorido ligand, which accelerated the benzylidene ligand dissociation.[18] However, the complex stability was found to be low, as indicated by the solution color change from green to brown during OM reactions. On the other hand, the sulfur atom in complex **4** directly coordinates to the metal center with an apparent 18-electron coordination fashion.[18] Despite this, the complex achieves final yields in OM reactions similar to those observed in complexes **1** and **3**. Unlike the case for *O*-coordinating complex **3**, *S*-coordinating complex **4** showed no change in solution color during OM reactions. Furthermore, it was found that complex **4** has a higher tolerance to protic solvents compared to complexes **1** and **3**. These observations highlighted different modes of reactivity regulation by chalcogen atoms (*O* and *S*) at the terminus of the phenoxy ether moiety. Expecting that heavier chalcogen atoms might reveal new modes of reactivity regulation for HG-II-type complexes, we investigated the effects of selenium (*Se*) atoms on the reactivities of HG-II-type complexes using a ruthenium complex containing a selenium atom at the terminus of the phenoxy ether moiety (complex **5**).[19]

Received: October 7, 2024
Revised: December 8, 2024
Accepted: December 10, 2024
Published: December 17, 2024

Chart 1. Structures of ruthenium complexes (1−5).

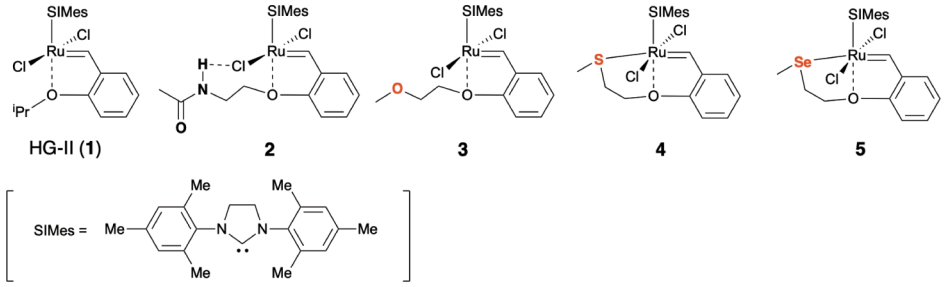

Scheme 1. Synthesis of Complex 5 Starting from 1,2-Dibromoethane and Salicylaldehyde

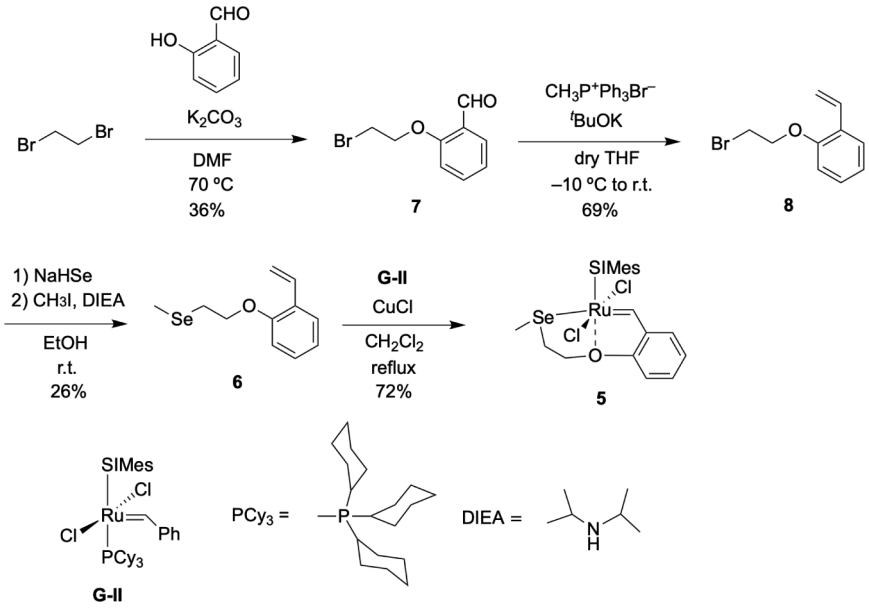

RESULTS AND DISCUSSION

Synthesis and Characterization of Selenoether-Containing Complex 5. The synthesis of complex **5** was performed according to the scheme shown in Scheme 1. Styrenyl selenoether ligand precursor **6** was obtained from salicylaldehyde in 3 steps: One bromide side of 1,2-dibromoethane was subjected to Williamson ether synthesis to yield compound **7**, which was subjected to a Wittig reaction to prepare compound **8**. Thereafter, a selenium atom was incorporated into the bromide moiety in compound **8**, followed by *in situ* methylation to prepare styrenyl selenoether **6**. Complex **5** was obtained through the reaction of compound **6** with Grubbs second-generation complex (G-II) in the presence of CuCl as a phosphine scavenger[5,20] and characterized using nuclear magnetic resonance (NMR) spectroscopy (Figures S1−S3) and mass analysis.

The ^{1}H NMR spectrum of complex **5** (Figure S1) showed the benzylidene proton signal at 16.3 ppm and the *Se*-methyl proton signal at 1.63 ppm. The *Se*-methyl proton signal was shifted upfield by 0.45 ppm compared to the *Se*-methyl protons in compound **6**. These spectral features are similar to those observed in *S*-containing complex **4**,[18] suggesting that complex **5** has a *trans*-configuration in the geometry of chlorido ligands, with *Se*-coordination to the metal center, akin to complex **4**. The *Se*-coordination was also suggested by the ^{77}Se-NMR spectrum with a signal at 114.2 ppm (Figure S3), which was shifted downfield from the signal observed in compound **6** (79.5 ppm). The X-ray crystallographic structure of complex **5** (Figure 1 and Table S1) confirmed *Se*-coordination with a

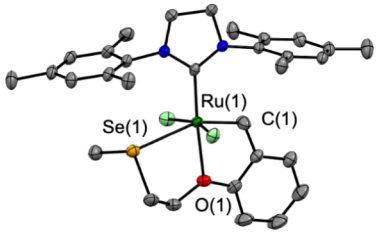

Figure 1. X-ray crystallographic structure of complex **5**. Thermal ellipsoids are drawn at the 50% possibility level. Selected bond lengths: Ru(1)−Se(1) 2.7875(5) Å; Ru(1)−C(1) 1.866(3) Å; Ru(1)−O(1) 2.236(1) Å.

Ru(1)−Se(1) bond distance of 2.7875(5) Å. The bond length is larger than the typical Ru−Se distances (∼ 2.45 Å) recorded in the Cambridge Crystallographic Data Center (CCDC) database, indicating a relatively weak *Se*-coordination in complex **5**. The *trans*-configuration observed in complex **5** sharply contrasts with a previously reported *Se*-coordinating Hoveyda-Grubbs-type complex, where the substitution of the phenolic oxygen in HG-II (**1**) with a selenium resulted in the *cis*-configuration.[11,19]

Ligand Exchange Reactions between HG-II (1) and Selenoether Ligand 6. Next, we investigated the effect of *Se*

https://doi.org/10.1021/acsomega.4c09137
ACS Omega 2024, 9, 51604−51610

Scheme 2. Ligand Exchange between HG-II (1) and Styrenyl Selenoether 6 to form Complex 5 and Styrenyl Ligand 9

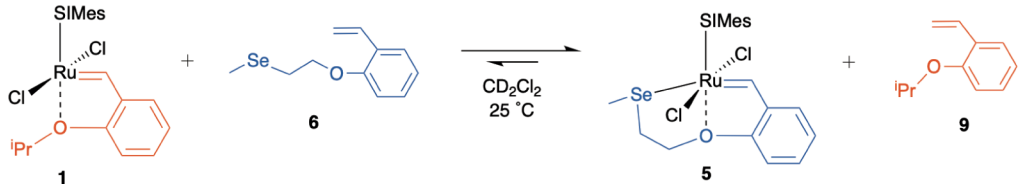

coordination on the relative thermodynamic stability of complex **5** against HG-II (**1**) using the stoichiometric ligand exchange reactions between HG-II (**1**) and ligand **6** (Scheme 2).[17,18] Yields of over 50% for complex **5** are equivalent to the higher thermodynamic stability of the complex than the parent HG-II (**1**). Monitoring the reaction using ^{1}H NMR over 48 h (Figures S4 and S5 ,Table S2) showed the formation of complex **5** in 95% yield along with the production of styrenyl ligand **9**. This fact indicates that *Se* coordination occurs in solutions as well as in the solid state, leading to the higher thermodynamic stability of complex **5** than HG-II (**1**).

OM Catalytic Activities. Our previous report showed that sulfur-coordinated complex **4** exhibits the catalytic reactivity of olefin metathesis despite a saturated coordination structure around the metal center.[18] Furthermore, its catalytic activity in the presence of protic solvents is higher than that of HG-II (**1**). Accordingly, we investigated the OM catalytic activity of complex **5** using the ring-closing metathesis (RCM) of *N*-tosyldiallylamide (TDA, **10**), a commonly used benchmark reaction for evaluating the reactivities of OM catalysts (Tables 1 and S3). The RCM reaction in 1,2-dichloroethane (1,2-DCE) was monitored by ^{1}H NMR spectroscopy (Figures S6 and S7). To examine the tolerance of complex **5** to protic media, the reactions were also conducted in the presence of methanol (Figures S8 and S9).

Table 1. RCM Reactions of TDA (10) Mediated by Ruthenium Catalysts[a]

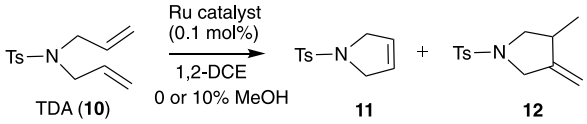

entry	catalyst	MeOH(%(v/v))	yield(%) 11	yield(%) 12
1	**1**	0	93 (0.3 h)[b], > 99 (6 h)[b,c]	N.D.[d]
2	**3**	0	89 (0.3 h)[b], 99 (6 h)[b,c]	N.D.[d]
3	**4**	0	53 (0.3 h)[b], 86 (6 h)[b,c]	N.D.[d]
4	**5**	0	12 (0.3 h), 95 (48 h)[c]	N.D.[d]
5	**1**	10	38 (12 h)[b,c]	trace (12 h)
6	**3**	10	19 (12 h)[b,c]	trace (12 h)
7	**4**	10	59 (48 h)[b,c]	7 (48 h)
8	**5**	10	47 (48 h)[c]	10 (48 h)

[a]reaction conditions: [**10**] = 42 mM and [complex] = 0.042 mM (0.1 mol % catalyst load) in 1,2-dichloroethane (1,2-DCE) at 40 °C. [b]quoted from ref.18 [c]yield when a reaction plateaued. [d]not detected.

In the absence of methanol, the complex **5**-mediated RCM reaction proceeded with a slower rate compared to other complexes (as seen by the yields at 0.3 h in entry 4 of Table 1), although the RCM product **11** ultimately reached a yield of ca. 90% at 48 h without forming cycloisomerized byproduct **12**. All investigated catalysts displayed a final RCM product yield of over 90% (entries 1−4 in Table 1). Additionally, in the presence of methanol, the **5**-catalyzed RCM reaction was slower than those mediated by other complexes (entry 8 vs entries 5−7). However, the final RCM product yield was higher than that in **1**- or **3**-catalyzed reactions (47% for **5** (entry 8); 38% for **1** (entry 5); and 19% for **3** (entry 6). The higher tolerance of complex **5** to methanol compared to complexes **1** and **3** was attributed to the *Se*-coordination similar to *S*-coordinated complex **4**. The coordinative selenoether ligand can protect the reactive intermediate from catalyst deactivation during the catalytic cycle as a release−return ligand (i.e., so-called "boomerang effect").[21] On the other hand, *Se*-coordinated complex **5** showed a lower RCM product yield compared to *S*-coordinated complex **4**. The byproduct yield increased slightly (7% for **4** and 10% for **5**).

Apart from the "boomerang effect" during the catalytic cycle, another possible reason for the higher tolerance of complex **5** to methanol is its intrinsic stability in MeOH-containing media. Previously, we have compared intrinsic stabilities of HG-II (**1**), *O*-coordinating complex **3**, and *S*-coordinating complex **4** in MeOH-containing media monitoring the changes in the ultraviolet−visible (UV−vis) spectra of these complexes *without* olefinic substrate molecules,[18] where the decrease in the metal-to-ligand charge transfer (MLCT) absorption band was observed. Accordingly, we monitored the UV−vis spectral changes of the complexes in MeOH-containing solution (Figure S10a− d) and compared the absorbance change at the maximum wavelengths of the MLCT bands (Figure S10e). Complex **5** exhibited an MLCT band at 390 nm. The wavelength is close to that of complex **4** (386 nm) and red-shifted from those of complexes **1** and **3** (**1**: 374 nm, **3**: 370 nm) because of *Se* coordination. As shown in Figure S10e, all of the complexes showed a decrease in the absorbance of the MLCT band in MeOH-containing solutions over 24 h; however, the extent of the absorbance changes was similar among the four complexes. This fact indicates that these complexes have similar intrinsic stabilities in MeOH-containing solution. Namely, the increased tolerance of complex **5** in MeOH-containing solutions is mainly due to participation of the released *Se*-containing styrenyl ligand in the catalytic cycle.

Moreover, we also examined the RCM of diethyl diallylmalonate (DDM (**13**)) and cross metathesis (CM) between 3-butenylbenzoate (**14**) and methyl acrylate (**15**) to investigate whether the reactivity tendency presented above is observed for other substrates and types of olefin metathesis.

In the RCM of DDM (Tables 2 and S4 Figure S11), all the catalysts produced RCM product **16** with more than 90% yields in the absence of methanol, where no isomerized product **17** was observed (Entries 1−4 in Table 2). Complexes **4** and **5** showed slower reaction velocities compared to those of complexes **1** and **3**, which is similar to that observed in the RCM reactions of TDA (**10**). In the presence of methanol, complexes **1** and **3** showed the decreased yields of the RCM

https://doi.org/10.1021/acsomega.4c09137
ACS Omega 2024, 9, 51604−51610

Table 2. RCM Reactions of DDM (13) Mediated by Ruthenium Catalysts[a]

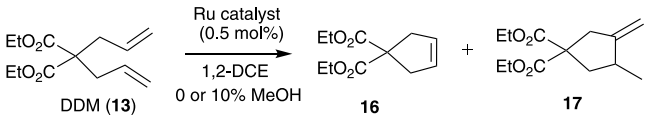

entry	catalyst	MeOH (%(v/v))	yield(%) 16	yield(%) 17
1	**1**	0	97 (6 h)[b]	N.D.[c]
2	**3**	0	>99 (1 h)[b]	N.D.[c]
3	**4**	0	97 (12 h)[b]	N.D.[c]
4	**5**	0	98 (12 h)[b]	N.D.[c]
5	**1**	10	39 (9 h)[b]	20 (9 h)[b]
6	**3**	10	22 (9 h)[b]	33 (9 h)[b]
7	**4**	10	71 (36 h)[b]	7 (36 h)
8	**5**	10	31 (30 h)[b]	8 (30 h)

[a]reaction conditions: [**13**] = 45 mM and [complex] = 0.225 mM (0.5 mol % catalyst load) in 1,2-dichloroethane (1,2-DCE) at 40° C. [b]yield when a reaction plateaued. [c]not detected.

product (>99% → 41% for **1**; > 99% → 22% for **3**), along with the formation of considerable amounts of isomerized compound **17**. Particularly, *O*-coordinated complex **2** produced more amount of isomerized compound **17** than RCM product **16**. In contrast, complexes **4** (*S*-coordination) and **5** (*Se*-coordination) mainly afforded the RCM product, even in the presence of methanol. *S*-coordinating complex **4** showed the moderate decrease in the yields in MeOH-containing solution (>97% → 71%; entries 3 vs. 7 in Table 2), resulting in the highest yields among the studied catalysts. This fact reflects the complex tolerance to methanol, as observed in the RCM of TDA (**10**). Complex **5** also showed a higher yield of RCM product **16** than *O*-coordinated complex **2** because of the increased tolerance to methanol provided by *Se* coordination.

In the CM reactions of 3-butenylbenzoate (**14**) with excess methyl acrylate (**15**) (**14**: **15** = 1:2; Tables 3 and S5 Figure S12), the reactions in the absence of methanol (Entries 1−4 in Table 3) showed similar final product yields among the complexes and slow reaction rates of **4**- and **5**-catalyzed reactions, as observed in the above-presented OM reactions. In MeOH-containing media, complexes **4** and **5** afforded higher product yields compared to complexes **1** and **2**. This is ascribed to the enhanced tolerance to methanol owing to the coordinative characteristic of the sulfur and selenium atoms in complexes **4** and **5**.

In whole, complex **4** tends to afford higher OM product yields than complex **5** in the presence of methanol. In other words, the reactivities of chalcogen-atom-containing catalysts (i.e., complexes **3** (*O*-containing), **4** (*S*-containing), and **5** (*Se*-containing)) do not simply follow the order of the periodic table. However, the enhanced tolerance of complexes **4** and **5** to methanol demonstrates the utility of coordinative atoms at the terminus of the phenoxy ether moiety for increasing the final yields of RCM products in the presence of protic solvents.

Kinetic Analyses for the Initial Phase in Catalytic Cycles. The chalcogen atom coordination to the metal center in complexes **4** and **5** may influence the initial phase of the OM catalytic cycle, as the dissociation of the chalcogen atom is involved in the activation of the precatalyst form. To evaluate the effects of chalcogen atom coordination on the initiation of OM catalytic cycles, we performed kinetic analyses of the reaction of OM catalysts with *n*-butyl vinyl ether (BuVE),[22−24] where the reaction produces a Fischer-type complex **20**, a catalytically inactive form and enables us to analyze the initial step of the catalytic cycle. The transient spectra observed in the presence of excess BuVE and pseudo-first-order kinetic plots are shown in Figures S13 and S14, respectively. The pseudo-first-order rate constants (k_{init}) at 25 °C for the reaction of Ru complexes with BuVE (Table 4) indicated smaller values for complexes **4** and **5** compared to those for complexes **1** and **3**. This is because the decoordination of the sulfur or selenium atom in the ligand is necessary for BuVE to access the metal center. The activation parameters of the reaction of Ru complexes with BuVE were determined by using Eyring plots shown in Figure S15. Complexes **1** and **3** exhibited more negative activation entropy ($\Delta S^{\ddagger}$) values compared to those of complexes **4** and **5**. HG-II (**1**) is known to mainly initiate OM catalytic cycles via "interchange mechanism" (i.e., substrate-binding along with the dissociation of the benzylidene ligand in the transition state).[23−25] Since complex **3** which contains an

Table 3. CM Reactions between 3-Butenylbenzoate (14) and Methyl Acrylate (15) and Mediated by Ruthenium Catalysts[a]

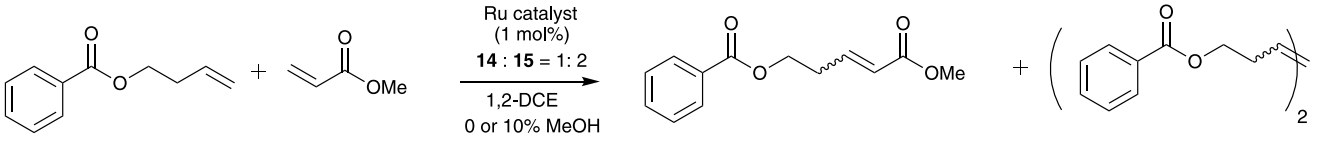

entry	catalyst	MeOH (%(v/v))	yield(%) 18	yield(%) 19
1	**1**	0	79 (12 h)[b,c]	4 (12 h)[b,d]
2	**3**	0	71 (24 h)[b,c]	7 (24 h)[b,d]
3	**4**	0	81 (36 h)[b,c]	6 (36 h)[b,d]
4	**5**	0	79 (36 h)[b,c]	6 (36 h)[b,d]
5	**1**	10	22 (24 h)[b,c]	3 (24 h)[b,d]
6	**3**	10	16 (24 h)[b,c]	4 (24 h)[b,d]
7	**4**	10	36 (36 h)[b,c]	7 (36 h)[b,d]
8	**5**	10	34 (48 h)[b,c]	7 (48 h)[b,d]

[a]reaction conditions: [**14**] = 42 mM and in [**15**] = 84 mM in 1,2-DCE; 1 mol % catalyst load; at 40° C. [b]yield when a reaction plateaued. [c]*E*/*Z* > 20/1. [d]*E*/*Z* > 20/1.

https://doi.org/10.1021/acsomega.4c09137
ACS Omega 2024, 9, 51604−51610

Table 4. Rate Constants (k_{init}) at 25 °C and Activation Parameters for the Reaction of n-Butyl Vinyl Ether (BuVE) with Ruthenium Complexes[a]

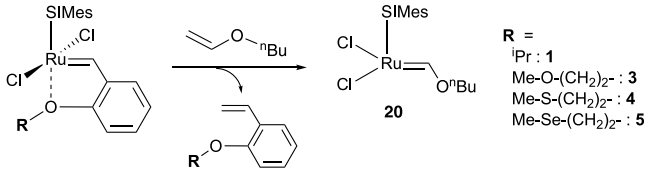

complex	$k_{initial}$[b] (M^{-1} s^{-1})	$\Delta H^{\ddagger}$ (kJmol^{-1})	$\Delta S^{\ddagger}$ (Jmol^{-1})
1	$(1.6 \pm 0.1) \times 10^{-2}$	64 ± 4[c] (59 ± 5[d])	−90 ± 10[c] (−78 ± 20[d])
3	$(4.6 \pm 0.3) \times 10^{-2}$	59 ± 6[c]	−96 ± 15[c]
4	$(3.2 \pm 0.2) \times 10^{-4}$	79 ± 3[c]	−51 ± 9[c]
5	$(1.8 \pm 0.1) \times 10^{-4}$	80 ± 8[c]	−50 ± 9[c]

[a]reaction conditions: [Ru complex] = 100 μM; in 1,2-dichloroethane (DCE). [b]rate constants obtained by pseudo-first-order kinetic analysis under excess BuVE ([BuVE] > 500 × [Ru complex]) at 25 °C. [c]average of three repeating experiments. [d]values in CH_2Cl_2 (quoted from ref;23 converted into joule unit).

oxygen in the ligand moiety but no *O*-metal coordination), showed similar activation parameters to HG-II (**1**), the "interchange mechanism" is the predominant pathway in the initial phase of **3**-catalyzed OM reactions. In contrast, complexes **4** and **5** displayed larger $\Delta H^{\ddagger}$ and $\Delta S^{\ddagger}$ values, reflecting the increased contribution of ligand dissociation in the initial step of the OM catalytic cycles. This fact indicates that the introduction of a sulfur or selenium atom at the terminus of the phenoxy ether moiety shifts the favorable mechanism in this step from the "interchange" pathway to a "dissociative" pathway.

CONCLUSION

In conclusion, the HG-II-type complex with a selenoether moiety in the benzylidene ligand exhibits the *Se*-coordination in its precatalyst form. The structural features result in the enhanced thermodynamic stability of the complex and greater tolerance to protic solvents compared to HG-II (**1**). A series of experimental results indicate that introducing coordinative atoms at the phenoxy ether moiety allows us to optimize OM reactivity, particularly in protic media, and to effectively regulate the reaction pathway in catalytic cycles. Since the solubilities of HG-type complexes in protic solvents can be increased by introducing ionic groups into the NHC ligand,[8,9,26,27] the findings of this study indicate the potential of HG-type complexes with a coordinative group in the phenoxy moiety as experimental tools for chemical modification of biomolecules in protic media.

METHODS

Materials. All chemicals were obtained from conventional commercial sources and used as received, unless otherwise noted. Hoveyda-Grubbs second generation catalyst (HG-II, **1**) and Grubbs second generation catalyst (**G-II**) were purchased from Sigma-Aldrich. Ruthenium complexes **3** and **4** were synthesized by previously reported methods.[18] Complex **5** and styrenyl selenoether ligand precursor **6** were synthesized according to the method described in the Supporting Information. *N*-Tosyldiallylamide (TDA, **10**)[28] and 3-butenylbezoate[29] were prepared according to the reported method. For silica gel chromatography, Wakosil C-200 (60−200 mesh) or Shodex purif-pack SI50 series were used.

Instruments. ^{1}H NMR (400 MHz), ^{13}C NMR (100 MHz), and ^{77}Se-NMR (76.2 MHz) spectra were collected by using a JEOL JNM-ECP 400 NMR spectrometer. ^{1}H NMR and ^{13}C NMR chemical shifts are reported in ppm relative to tetramethylsilane (TMS). ^{77}Se-NMR chemical shifts were determined based on diphenyl diselenide (Ph−Se−Se-Ph. δ_{Se} = 480 ppm). ESI-MS analyses were carried out using a JEOL JMS-T100LC mass spectrometer. EI- and CI-MS analyses were conducted by using a JEOL JMS-700 MStation spectrophotometer. UV−vis spectra were measured using a Shimadzu UV-2550 spectrophotometer equipped with a thermostated folder. X-ray crystallographic data were collected on a Rigaku AXIS-RAPID Imaging Plate diffractometer and analyzed by using SHELXL-2019/2.

X-ray Crystallographic Analysis of Complex 5. A single crystal of complex **5** was prepared by vapor diffusion of hexane into a CH_2Cl_2 solution at 5 °C. X-ray diffraction was collected at 125 ± 0.1 K. The crystal data, diffraction collection details, and structure refinement are given in Table S1. The crystallographic data were deposited in Cambridge Crystallographic Data Center (CCDC).

Ligand Exchange Reactions between HG-II (1) and Ligand 6. Sample preparation was conducted in a N_2-filled glovebox. HG-II (**1**), ligand **6**, and hexamethyldisiloxane (HMDSO, internal standard) were dissolved in 600 μL of dried/degassed CD_2Cl_2 ([**1**] = [ligand] = 50 mM; [HMDSO] = 5 mM in final). The solution was transferred into an NMR tube with a J. Young screw cap, and the reaction at 25 °C in the dark was monitored by ^{1}H NMR measurements with presaturation technique for the undeuterated protons in solvent. The reactants and products were quantified using eq 1 shown below:

$$C_{rxn} = (I_{rxn}/I_{IS}) \times (H_{IS}/H_{rxn}) \times C_{IS} \quad (1)$$

, where

C_{rxn}: concentration of a reactant or product

I_{rxn}: NMR signal intensity of the monitored peak for a reactant or product (see below)

I_{IS}: NMR signal intensity of the peak from an internal standard

H_{IS}: the number of protons in an internal standard

H_{rxn}: the number of protons in the monitored peak for a reactant or product

C_{IS}: concentration of an internal standard.

In this case, H_{IS} = 18 and C_{IS} = 5 mM. The peaks observed for reactants are as follows: HG-II (**1**) (4.87 ppm, 1H, $(CH_3)_2C\underline{H}O-$); complex **5** (1.63 ppm, 3H, $C\underline{H_3}SeCH_2CH_2O-$); ligand **6** (2.92 ppm, 2H,

https://doi.org/10.1021/acsomega.4c09137
ACS Omega 2024, 9, 51604−51610

$CH_3SeC\underline{H}_2CH_2O-$); ligand **9** (4.55 ppm, 1H, $(CH_3)_2C\underline{H}O-$). The material balance was checked throughout the reaction by monitoring the sum of [HG-II (**1**)] + [product complex **5**] and [reacting ligand **6**] + [product ligand **9**]. The experimental data are presented based on the average of experiments repeated three times.

Ring-Closing Metathesis (RCM) of TDA (10). In a 20 mL Schlenk tube, TDA (**10**) (42 mM) was dissolved in dry/degassed 1,2-dichloroethane (1,2-DCE) or methanol-containing 1,2-DCE (10% MeOH(v/v)). After a Ru catalyst was added (0.1 mol % load), the RCM reaction was conducted at 40 °C in the dark. At defined times, an aliquot of solution (100 μL) was sampled, and ethyl vinyl ether was added to quench the reaction. Thereafter, the solvent was evaporated, and 600 μL of dimethylsulfone (DMS; an internal standard; δ_H = 2.99 ppm) in $CDCl_3$ (3 mM) was added. The solution was subjected to ^{1}H NMR measurements to quantify the reaction components based on eq 1. In this case, H_{IS} = 6 and C_{IS} = 3 mM. The monitored peaks for the products are as follows: RCM product **11** (4.12 ppm, 4H, -NC$\underline{H}_2$-CH =), and isomerized product **12** (1.04 ppm, 3H, > CH-C$\underline{H}_3$).[30] The experimental data are presented based on the average of experiments repeated three times.

Ring-Closing Metathesis (RCM) Reactions of DDM (13). Sample preparation and reactions were conducted in the same manner as described above except for the use of 0.5 mol % catalyst load. After sampling an aliquot of solution (100 μL) at defined time, the solution was diluted with 500 μL of $CDCl_3$ that contains HMDSO (internal standard, 0.234 mM in final), which was subjected to ^{1}H NMR measurements with the presaturation technique for signals derived from 1,2-DCE (3.74 ppm). The quantification of DDM and products was conducted based on eq 1, where H_{IS} = 18 and C_{IS} = 0.2 mM. The monitored peaks for products are as follows: RCM product **16** (3.00 ppm, 4H, $(EtO_2C)_2$-C-(C$\underline{H}_2$-CH =)$_2$); isomerized product **17** (1.08 ppm, 3H, > CH-C$\underline{H}_3$).[30]

Cross Metathesis (CM) Reactions between 3-Butenylbenzoate (14) and Methyl Acrylate (15). Sample preparation, reactions, and quantification of reaction components were conducted in the same manner as for the RCM reactions of DDM (**13**). The concentration of a Ru catalyst was set to 1 mol % of DDM concentration. The monitored peaks for products are as follows: hetero-CM product **18** (4.44 ppm, 2H, -OC$\underline{H}_2$-CH_2−CH =), and self-CM product (derived from **15**) **19** (4.32 ppm, 4H, -OC$\underline{H}_2$-CH_2−CH =).[31,32]

Kinetic Measurements of Initial Phases in Olefin Metathesis reactions.[22−24] Sample preparation was conducted in a N_2-filled glovebox. A solution of a ruthenium catalyst in 1,2-DCE was charged into a quartz cell equipped with a septum cap and incubated at the desired temperatures. After a solution of *n*-butyl vinyl ether (BuVE) was added to the Ru complex solution with a syringe, the absorbance in the metal-to-ligand charge transfer (MLCT) band (378 nm for HG-II (**1**); 372 nm for **3**; 391 nm for **4**; 395 nm for **5**) was monitored. The final concentrations of the reactants were set as follows: [Ru complex] = 2 × 10^{-4} M and [BuVE] = 0.005 M−0.3 M (for HG-II (**1**) and **3**), 0.05 M 0.3 M (for **4**), or 0.05 M−0.6 M (for **5**), where pseudo-first-order kinetic conditions were kept. The changes in the absorbance were analyzed by eq 2:

$$k_{obs} = k_{initial} \bullet [BuVE] \quad (2)$$

where k_{obs} is an apparent pseudo-first-order rate constant and $k_{initial}$ is the rate constant of the initial phase in the catalytic cycle.

At the lowest concentrations of BuVE, the transient spectra in the range from 250 to 700 nm were also recorded to confirm UV−vis spectral changes with isosbestic points. To obtain activation parameters, pseudo-first-order kinetic constants at constant BuVE concentrations were plotted against the reciprocal of temperatures (Eyring plot) and analyzed using eq 3:

$$ln(k_{obs}/T) = -(\Delta H^{\ddagger}/R) \bullet (1/T) + ln(k_B/h) + \Delta S^{\ddagger}/R \quad (3)$$

where T is temperature; $\Delta H^{\ddagger}$is the activation enthalpy; R is the gas constant; k_B is Boltzmann constant; h is Planck constant; $\Delta S^{\ddagger}$ is the activation entropy. The experimental data are presented based on the average of experiments repeated three times.

■ ASSOCIATED CONTENT

Supporting Information

The Supporting Information is available free of charge at https://pubs.acs.org/doi/10.1021/acsomega.4c09137.

Crystallographic data for complex **5**(CIF)

Synthetic procedures, X-ray crystallographic data, NMR spectra of complex **5**, NMR spectral changes during ligand exchange, quantification of ligand exchange and olefin metathesis reactions, UV−vis spectra, and kinetic analyses (PDF)

■ AUTHOR INFORMATION

Corresponding Author

Takashi Matsuo − *Division of Materials Science, Nara Institute of Science and Technology, Ikoma, Nara 630-0192, Japan*; orcid.org/0000-0002-5646-6251; Email: matsuo.takashi@naist.ac.jp

Authors

Tsubasa Kinugawa − *Division of Materials Science, Nara Institute of Science and Technology, Ikoma, Nara 630-0192, Japan*

Seishu Mitsusada − *Division of Materials Science, Nara Institute of Science and Technology, Ikoma, Nara 630-0192, Japan*

Naoki Orito − *Division of Materials Science, Nara Institute of Science and Technology, Ikoma, Nara 630-0192, Japan*

Complete contact information is available at: https://pubs.acs.org/10.1021/acsomega.4c09137

Author Contributions

T.K., S.M., and N.O.: Investigation; Resources; Visualization; Writing−review and editing; T.M.: Conceptualization; Funding acquisition; Investigation; Project administration; Resources; Supervision; Visualization; Writing−review and editing.

Notes

The authors declare no competing financial interest.

■ ACKNOWLEDGMENTS

This work was supported by a Grant-in-Aid for Scientific Research (C) (JSPS KAKENHI grant number JP22K05316). The authors thank Mr. Shohei Katao for X-ray crystallographic analysis, Mr. Fumio Asanoma for the support of NMR

measurements and Prof. Shun Hirota for his kind arrangement of our facility usage.

REFERENCES

(1) Grubbs, R. H.; Trnka, T. M. Ruthenium-Catalyzed Olefin Metathesis. In *Ruthenium in Organic Synthesis*; Wiley-VCH Verlag GmbH & Co. KGaA, 2004; pp. 153−177.
(2) Levin, E.; Ivry, E.; Diesendruck, C. E.; Lemcoff, N. G. Water in N-Heterocyclic Carbene-Assisted Catalysis. *Chem. Rev.* **2015**, *115* (11), 4607−4692.
(3) Hughes, D.; Wheeler, P.; Ene, D. Olefin Metathesis in Drug Discovery and Development—Examples from Recent Patent Literature. *Org. Process Res. Dev.* **2017**, *21* (12), 1938−1962.
(4) Lecourt, C.; Dhambri, S.; Allievi, L.; Sanogo, Y.; Zeghbib, N.; Ben Othman, R.; Lannou, M. I.; Sorin, G.; Ardisson, J. Natural Products and Ring-Closing Metathesis: Synthesis of Sterically Congested Olefins. *Nat. Prod. Rep.* **2018**, *35* (1), 105−124.
(5) Garber, S. B.; Kingsbury, J. S.; Gray, B. L.; Hoveyda, A. H. Efficient and Recyclable Monomeric and Dendritic Ru-Based Metathesis Catalysts. *J. Am. Chem. Soc.* **2000**, *122* (34), 8168−8179.
(6) Ingram, A. A.; Wang, D.; Schwaneberg, U.; Okuda, J. Grubbs-Hoveyda Catalysts Conjugated to a β-Barrel Protein: Effect of Halide Substitution on Aqueous Olefin Metathesis Activity. *J. Inorg. Biochem.* **2024**, *258*, 112616.
(7) Blanco, C. O.; Ramos Castellanos, R.; Fogg, D. E. Anionic Olefin Metathesis Catalysts Enable Modification of Unprotected Biomolecules in Water. *ACS Catal.* **2024**, *14* (15), 11147−11152.
(8) Szczepaniak, G.; Kosiński, K.; Grela, K. Towards "Cleaner" Olefin Metathesis: Tailoring the NHC Ligand of Second Generation Ruthenium Catalysts to Afford Auxiliary Traits. *Green Chem.* **2014**, *16* (10), 4474−4492.
(9) Matsuo, T. Functionalization of Ruthenium Olefin-Metathesis Catalysts for Interdisciplinary Studies in Chemistry and Biology. *Catalysts* **2021**, *11* (3), 359.
(10) Nadirova, M.; Zieliński, A.; Malinska, M.; Kajetanowicz, A. Fast Initiating Furan-Containing Hoveyda-Type Complexes: Synthesis and Applications in Metathesis Reactions. *Chemistry* **2022**, *4* (3), 786−795.
(11) Antonova, A. S.; Zubkov, F. I. Hoveyda-Grubbs Type Complexes with Ruthenium-pnictogen/halcogen/halogen Coordination Bond. Synthesis, Catalytic Activity, Applications. *Russ. Chem. Rev.* **2024**, *93* (8), RCR5132.
(12) Czarnocki, S. J.; Czeluśniak, I.; Olszewski, T. K.; Malinska, M.; Woźniak, K.; Grela, K. Rational and Then Serendipitous Formation of Aza Analogues of Hoveyda-Type Catalysts Containing a Chelating Ester Group Leading to a Polymerization Catalyst Family. *ACS Catal.* **2017**, *7* (6), 4115−4121.
(13) Hejl, A.; Day, M. W.; Grubbs, R. H. Latent Olefin Metathesis Catalysts Featuring Chelating Alkylidenes. *Organometallics* **2006**, *25* (26), 6149−6154.
(14) Bieniek, M.; Bujok, R.; Cabaj, M.; Lugan, N.; Lavigne, G.; Arlt, D.; Grela, K. Advanced Fine-Tuning of Grubbs/Hoveyda Olefin Metathesis Catalysts: A Further Step toward an Optimum Balance between Antinomic Properties. *J. Am. Chem. Soc.* **2006**, *128* (42), 13652−13653.
(15) Gawin, R.; Makal, A.; Woźniak, K.; Mauduit, M.; Grela, K. A Dormant Ruthenium Catalyst Bearing a Chelating Carboxylate Ligand: In Situ Activation and Application in Metathesis Reactions. *Angew. Chem., Int. Ed.* **2007**, *46* (38), 7206−7209.
(16) Pump, E.; Fischer, R. C.; Slugovc, C. Halide Exchange in Second-Generation cis-Dihalo Ruthenium Benzylidene Complexes. *Organometallics* **2012**, *31* (19), 6972−6979.
(17) Jatmika, C.; Goshima, K.; Wakabayashi, K.; Akiyama, N.; Hirota, S.; Matsuo, T. Second-Coordination Sphere Effects on the Reactivities of Hoveyda-Grubbs-type Catalysts: A Ligand Exchange Study Using Phenolic Moiety-Functionalized Ligands. *Dalton Trans.* **2020**, *49* (33), 11618−11627.
(18) Kinugawa, T.; Matsuo, T. Reactivity Regulation for Olefin Metathesis-Catalyzing Ruthenium Complexes with Sulfur Atoms at the Terminal of 2-Alkoxybenzylidene Ligands. *Dalton Trans.* **2023**, *52* (27), 9499−9508.
(19) A previous report on selenium-coordinating Hoveyda-Grubbs-type complex: Monsigny, L.; Cejas Sánchez, J.; Piątkowski, J.; Kajetanowicz, A.; Grela, K. Synthesis and Catalytic Properties of a Very Latent Selenium-Chelated Ruthenium Benzylidene Olefin Metathesis Catalyst. *Organometallics* **2021**, *40* (21), 3608−3616.
(20) Ledoux, N.; Linden, A.; Allaert, B.; Mierde, H. V.; Verpoort, F. Comparative Investigation of Hoveyda−Grubbs Catalysts Bearing Modified N-Heterocyclic Carbene Ligands. *Adv. Synth. Catal.* **2007**, *349* (10), 1692−1700.
(21) Bates, J. M.; Lummiss, J. A. M.; Bailey, G. A.; Fogg, D. E. Operation of the Boomerang Mechanism in Olefin Metathesis Reactions Promoted by the Second-Generation Hoveyda Catalyst. *ACS Catal.* **2014**, *4* (7), 2387−2394.
(22) Vorfalt, T.; Wannowius, K.-J.; Plenio, H. Probing the Mechanism of Olefin Metathesis in Grubbs−Hoveyda and Grela Type Complexes. *Angew. Chem. Int. Ed.* **2010**, *49* (32), 5533−5536.
(23) Ashworth, I. W.; Hillier, I. H.; Nelson, D. J.; Percy, J. M.; Vincent, M. A. What is The Initiation Step of the Grubbs-Hoveyda Olefin Metathesis Catalyst? *Chem. Commun.* **2011**, *47* (19), 5428−5430.
(24) Thiel, V.; Hendann, M.; Wannowius, K.-J.; Plenio, H. On the Mechanism of the Initiation Reaction in Grubbs−Hoveyda Complexes. *J. Am. Chem. Soc.* **2012**, *134* (2), 1104−1114.
(25) Nelson, D. J.; Manzini, S.; Urbina-Blanco, C. A.; Nolan, S. P. Key Processes in Ruthenium-Catalysed Olefin Metathesis. *Chem. Commun.* **2014**, *50* (72), 10355−10375.
(26) Jordan, J. P.; Grubbs, R. H. Small-Molecule N-Heterocyclic-Carbene-Containing Olefin-Metathesis Catalysts for Use in Water. *Angew. Chem., Int. Ed.* **2007**, *46* (27), 5152−5155.
(27) Hong, S. H.; Grubbs, R. H. Highly Active Water-Soluble Olefin Metathesis Catalyst. *J. Am. Chem. Soc.* **2006**, *128* (11), 3508−3509.
(28) Varray, S.; Lazaro, R.; Martinez, J.; Lamaty, F. New Soluble-Polymer Bound Ruthenium Carbene Catalysts: Synthesis, Characterization, and Application to Ring-Closing Metathesis. *Organometallics* **2003**, *22* (12), 2426−2435.
(29) Bogen, S.; Arasappan, A.; Pan, S.; Ruan, S.; Padilla, A.; Saksena, A. K.; Girijavallabhan, X.; Njoroge, F. G. Hepatitis C Virus NS3−4A Serine Protease Inhibitors: SAR of New P1 Derivatives of SCH 503034. *Bioorg. Med. Chem. Lett.* **2008**, *18* (14), 4219−4223.
(30) Lexer, C.; Burtscher, D.; Perner, B.; Tzur, E.; Lemcoff, N. G.; Slugovc, C. Olefin metathesis catalyst bearing a chelating phosphine ligand. *J. Org. Chem.* **2011**, *696* (11), 2466−2470.
(31) Schmid, T. E.; Bantreil, X.; Citadelle, C. A.; Slawin, A. M. Z.; Cazin, C. S. J. Phosphites as Ligands in Ruthenium-benzylidene Catalysts for Olefin Metathesis. *Chem. Commun.* **2011**, *47* (25), 7060−7062.
(32) Rix, D.; Caijo, F.; Laurent, I.; Boeda, F.; Clavier, H.; Nolan, S. P.; Mauduit, M. Aminocarbonyl Group Containing Hoveyda−Grubbs-Type Complexes: Synthesis and Activity in Olefin Metathesis Transformations. *J. Org. Chem.* **2008**, *73* (11), 4225−4228.

https://doi.org/10.1021/acsomega.4c09137
ACS Omega 2024, 9, 51604−51610